

Primary structure of N-linked carbohydrate chains of a human chimeric plasminogen activator K₂tu-PA expressed in Chinese hamster ovary cells

Aldert A. BERGWERFF¹, Jan van OOSTRUM², Fred A. M. ASSELBERGS², Rolf BÜRGI², Cornelis H. HOKKE¹,
Johannis P. KAMERLING¹ and Johannes F. G. Vliegenthart¹

¹ Bijvoet Center, Department of Bio-Organic Chemistry, Utrecht University, The Netherlands

² Ciba-Geigy Ltd, Department of Biotechnology, Basel, Switzerland

(Received August 4, 1992) – EJB 92 1130

A recombinant human plasminogen activator hybrid variant K₂tu-PA, expressed in Chinese hamster ovary cells, is partially glycosylated at Asn12 (A chain, kringle-2 domain) and completely glycosylated at Asn247 (B chain, protease domain). After release of the N-linked carbohydrate chains by peptide-N⁴-(*N*-acetyl- β -glucosaminy)l-asparagine amidase F, the oligosaccharides were separated from the protein by gel permeation chromatography, then fractionated by FPLC on Mono Q, followed by HPLC on Lichrosorb-NH₂, and analysed by 500-MHz ¹H-NMR spectroscopy. The following types of carbohydrates occur: monosialylated diantennary (8%), disialylated diantennary (45%), disialylated tri- and tri'-antennary (1%), trisialylated tri- and tri'-antennary (28%), and tetrasialylated tetra-antennary (18%) structures, all having fucose in α (1-6)-linkage at the Asn-bound *N*-acetylglucosamine. Sialic acid occurred exclusively in α (2-3)-linkage to galactose, and consisted of *N*-acetylneuraminic acid (94%), *N*-glycolylneuraminic acid (3%), and *N*-acetyl-9-*O*-acetylneuraminic acid (3%). In addition, glycopeptide fragments corresponding with the A or B chain of K₂tu-PA were analysed. The oligosaccharides attached to Asn12 are less processed than those attached to Asn247. Comparison of the glycosylation pattern of K₂tu-PA with that of tissue-type plasminogen activator from different biological sources showed significant differences.

Profiling studies on different K₂tu-PA production batches demonstrated that the structures of N-linked oligosaccharides were identical, but that relative amounts vary with the applied isolation procedure of the chimeric glycoprotein.

Plasminogen activators (PA) are serine proteases, that convert the inactive proenzyme plasminogen into the active enzyme plasmin, thereby functioning as important initiators of fibrinolysis. Two types of plasminogen activators can be distinguished, namely, the urinary-type (urokinase, u-PA) and the tissue-type (t-PA) [1]. Urokinase and recombinant t-PA are of clinical interest for the treatment of acute vascular diseases like myocardial infarction [2–4]. To obtain artery reperfusion, high blood levels of PA are required, because of its rapid clearance by the liver. Such pharmaceutical use is associated with a variable degree of systemic fibrinolytic ac-

tivation, fibrinogen breakdown, and bleeding tendency (e. g. cerebral haemorrhages) [2, 3, 5]. Therefore, more effective and safe fibrinolytic agents are of high interest [6].

Human type I t-PA contains N-linked carbohydrate chains at Asn117 (kringle-1 domain), Asn184 (kringle-2 domain), and Asn448 (serine protease domain), whereas human type II t-PA has N-linked carbohydrate chains at Asn117 and Asn448 [7]. In t-PA from human colon fibroblast and Bowes melanoma cells, the oligosaccharides bound to Asn117 are predominantly of the oligomannose type [8]. The oligosaccharides at Asn184 and Asn448 comprise predominantly *N*-acetylglucosamine type of structures in the case of human colon fibroblast cells [8], and contain predominantly GalN-Ac β 1-4GlcNAc elements in the case of Bowes melanoma cells [9]. The presence and the nature of the N-linked carbohydrate chains in t-PA have been reported to play a role in various biological phenomena [10–12]. Glycosylation at Asn184 inhibits the conversion of single-chain to two-chain t-PA by plasmin [13], which cleaves the polypeptide backbone of t-PA between Arg275 and Ile276 [7]. N-linked carbohydrate chains of human u-PA are located only at the protease domain (Asn302), and contain at least four GlcNAc and two GalNAc residues [14]. Furthermore, the presence of mucin-type O-linked oligosaccharides has been suggested [15]. Recently, O-linked fucose (Fuc) has been shown to be attached to Thr61 of t-PA [16] and to Thr18 of u-PA [17], both located in the epidermal growth factor-like domains.

Correspondence to J. P. Kamerling, Bijvoet Center, Department of Bio-Organic Chemistry, Utrecht University, P. O. Box 80.075, NL-3508 TB Utrecht, The Netherlands

Abbreviations. PNGase-F, peptide-N⁴-(*N*-acetyl- β -glucosaminy)l-asparagine amidase F; PA, plasminogen activator; u-PA, urinary-type plasminogen activator; t-PA, tissue-type plasminogen activator; CHO, Chinese hamster ovary; Neu5Ac, *N*-acetylneuraminic acid; Neu5Gc, *N*-glycolylneuraminic acid; Neu5,9Ac₂, *N*-acetyl-9-*O*-acetylneuraminic acid; 1D, one-dimensional; 2D, two-dimensional; HOHAHA, homonuclear Hartmann-Hahn; MLEV, composite pulse devised by Malcolm Levitt; COSY, scalar shift correlated spectroscopy; ROESY, rotating-frame nuclear Overhauser enhancement spectroscopy.

Enzymes. Peptide-N⁴-(*N*-acetyl- β -glucosaminy)l-asparagine amidase F (EC 3.5.1.52); urinary-type and tissue-type plasminogen activator (EC 3.4.21.31).

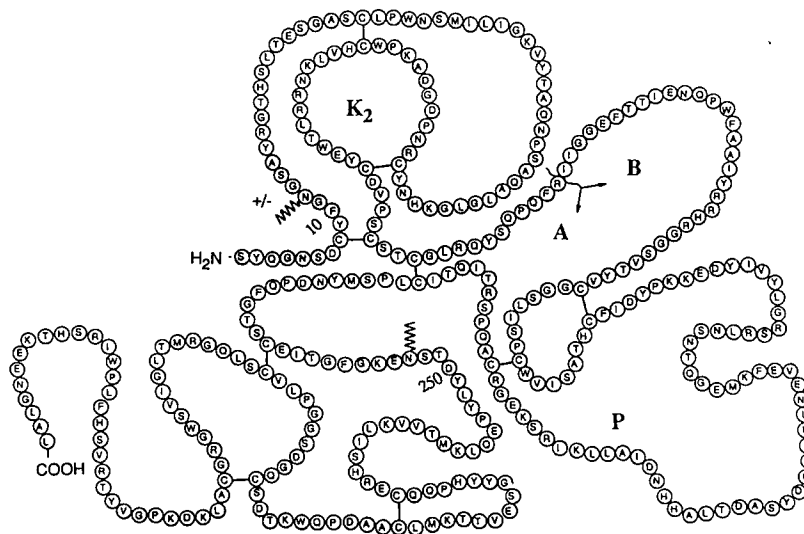


Fig. 1. Diagram of the amino acid sequence of K_2 tu-PA. The plasmin cleavage site is indicated and splits K_2 tu-PA into an A chain and a B chain. The zig-zags denote positions of N-linked oligosaccharide; K_2 , kringle-2 domain; P, serine protease domain.

Both u-PA and t-PA are mosaic glycoproteins containing individual protein domains with autonomous functions, namely, signal peptide (SP), pro-sequence (PS), a finger (F), epidermal growth factor (EGF), kringle (K), and serine protease (P) domains, so that t-PA can be written as SP-PS-F-EGF- K_1 - K_2 -P, and u-PA as SP-EGF-K-P [18, 19]. The protein domains are encoded by separate exons or sets of exons. Using the 'exon-shuffling' model [20], efforts have been made to obtain improved PA variants by protein engineering techniques, the so-called second generation plasminogen activators (for examples, see [18, 19, 21]). In this context, a hybrid variant K_2 tu-PA has been constructed, wherein sequences coding for the kringle-2 domain of t-PA and for the protease domain of u-PA, were combined on the gene level [22]. For the expression, Chinese hamster ovary (CHO) cells were chosen, an obvious choice from a carbohydrate point of view, since glycoproteins synthesised by these cells have oligosaccharides which are predominantly closely related to those found in man [23, 24].

The chimeric glycoprotein (Fig. 1) is partially glycosylated at Asn12 (originally Asn184 of t-PA) and completely glycosylated at Asn247 (originally Asn302 of u-PA). This study presents the fractionation and structure determination of the enzymically released N-linked oligosaccharides of K_2 tu-PA. To obtain information about the type of carbohydrate chains at each glycosylation site, profiling studies were carried out on the A chain (kringle-2 domain) and B chain (protease domain), derived from K_2 tu-PA. In addition, profiling studies were performed for batch control of K_2 tu-PA preparations, and the results will be discussed.

EXPERIMENTAL PROCEDURES

Materials

Peptide- N^A -(*N*-acetyl- β -glucosaminyl)asparagine amidase F (PNGase-F) from *Flavobacterium meningosepticum* was purchased from Boehringer Mannheim (FRG). Neu5,9Ac₂-6Gal β 1-4GlcNAc was a gift of Dr. C. Augé (Institut de Chimie Moléculaire d'Orsay, Université Paris-Sud, France). Urine from female Wistar rats was provided by the Gemeensch-

appelijk Dierenlaboratorium of Utrecht University. Carbobenzoyglycyl-glycyl-L-arginine-7-amino-4-methylcoumarin (Cbz-Gly-Gly-Arg-NH-Mec) was purchased from Bachem (Dubendorf, Switzerland).

Expression of K_2 tu-PA, cultivation of CHO cells, and isolation of K_2 tu-PA

Briefly, the production of the batches CGI-1/3 (K_2 tu-PA-I), 9005 (K_2 tu-PA-II), 9006 (K_2 tu-PA-III), and 113079 (K_2 tu-PA-IV) was as follows. The gene for the hybrid K_2 tu-PA was constructed from the relevant cDNAs of the parental t-PA and u-PA, and inserted in the expression plasmid pCGA72a [22]. In this plasmid, the expression of foreign DNA is driven by the immediate-early promoter of mouse cytomegalovirus, containing the dihydrofolate reductase (*dhfr*) gene. The plasmid was used to transfect *dhfr*⁻ CHO cells (recombinant cell line CHO-CGI-1) [25]. High-producing clones were selected after methotrexate-induced DNA amplification, using ELISA techniques to quantify K_2 tu-PA [22]. K_2 tu-PA-II and -III were produced by cells having the same passage and almost identical handling history. K_2 tu-PA-IV was produced under identical fermentation conditions, but a year earlier.

K_2 tu-PA-I was obtained from four subsequent harvests of a fed batch culture from a 10-l stirred tank bioreactor. For the cultivation, a basal production medium was supplemented with 1% (by vol.) fetal calf serum, 0.1% (by mass) bovine albumin, 5 μ g/ml bovine insulin, and 5 μ g/ml human transferrin. Finally, 10 KIU/ml aprotinin and 25 mM 6-aminohexanoic acid were added to inhibit residual plasmin activity. K_2 tu-PA-II, -III and -IV were produced in a 100-l perfusion chemostat bioreactor under the same conditions as for K_2 tu-PA-I, except that the basal medium was supplemented with 1% (by vol.) fetal calf serum, 6 μ g/ml insulin, 30 μ g/ml bovine transferrin, 10 KIU/ml aprotinin and 10 mM 6-aminohexanoic acid.

Batch K_2 tu-PA-I was purified by column chromatography, using Mab405-B-33-3 coupled to CNBr-activated Sepharose-4B (Pharmacia); the monoclonal antibody recognizes an epitope on the kringle-2 domain of t-PA [22]. After extensive washing with 2 M NaCl, the column was eluted

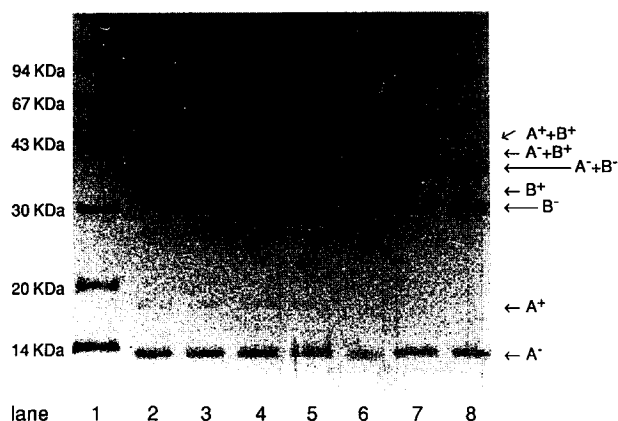


Fig. 2. SDS/PAGE of K_2 tu-PA on a 12.5% slab gel, 2.6% cross-linking. Lane 1, molecular mass markers; lane 2, intact K_2 tu-PA. Lanes 3–6, addition of 0.5 U PNGase-F/mg K_2 tu-PA and analysis, after 30 min, 1 h, 1.5 h, and 2 h, respectively. Lanes 7 and 8, addition of extra 0.4 U PNGase-F/mg K_2 tu-PA after 2 h and 18 h, and analysis after 18 h and 24 h, respectively. Each lane contains 5 μ g protein. $A^+ + B^+$, glycosylated A with glycosylated B chain; $A^- + B^+$, non-glycosylated A with glycosylated B chain; $A^- + B^-$, de-N-glycosylated A with B chain; B^+ , glycosylated B chain; B^- , de-N-glycosylated B chain; A^+ , glycosylated A chain; A^- , non- and/or de-N-glycosylated A chain.

with 100 mM 6-aminohexanoic acid, adjusted to pH 2.0 with HCl, and collected fractions were immediately adjusted to pH 6.0 with 1 M Tris. The fractions containing K_2 tu-PA-I, as traced by a direct amidolytic assay with Cbz-Gly-Gly-Arg-NH-Mec as fluorogenic substrate [26], were pooled and loaded on a S-Sepharose FF cation-exchange column (Pharmacia), equilibrated in 50 mM sodium phosphate pH 6.0. The column was eluted with a linear gradient of 0–500 mM NaCl in 50 mM sodium phosphate pH 6.0. The fractions containing K_2 tu-PA-I (amidolytic assay) were pooled and stored at -80°C , after dialysis against 25 mM sodium acetate pH 5.0.

The culture media from the K_2 tu-PA-II, -III and -IV batches were processed applying a multistep purification protocol, which includes cation- and anion-exchange chromatography, and hydrophobic interaction chromatography on aminohexyl-Sepharose (Pharmacia). Subsequently, *p*-aminobenzamidine-agarose, which binds active serine proteases, was used to remove small amounts of two-chain K_2 tu-PA. Finally, the material was submitted to a column of Sephadex G-50, eluted with 25 mM sodium succinate pH 4.0 (K_2 tu-PA-II and -III) or 25 mM sodium acetate pH 5.0 (K_2 tu-PA-IV), and the fractions containing K_2 tu-PA were pooled and stored at -80°C .

Preparation and isolation of A and B chain from K_2 tu-PA

To obtain K_2 tu-PA completely in the two-chain form (cf. Fig. 1), K_2 tu-PA-IV was incubated with plasmin, coupled to CNBr-activated Sepharose, for 2.5 h at ambient temperature. After reduction and carboxymethylation [27], the A and B chains were separated on a Nucleosil C_{18} reverse-phase HPLC column, eluted with a linear gradient of 30–50% (by vol.) acetonitrile in water, containing 0.1% trifluoroacetic acid. The fractions containing the A or B chain, as judged from SDS/PAGE, were lyophilised.

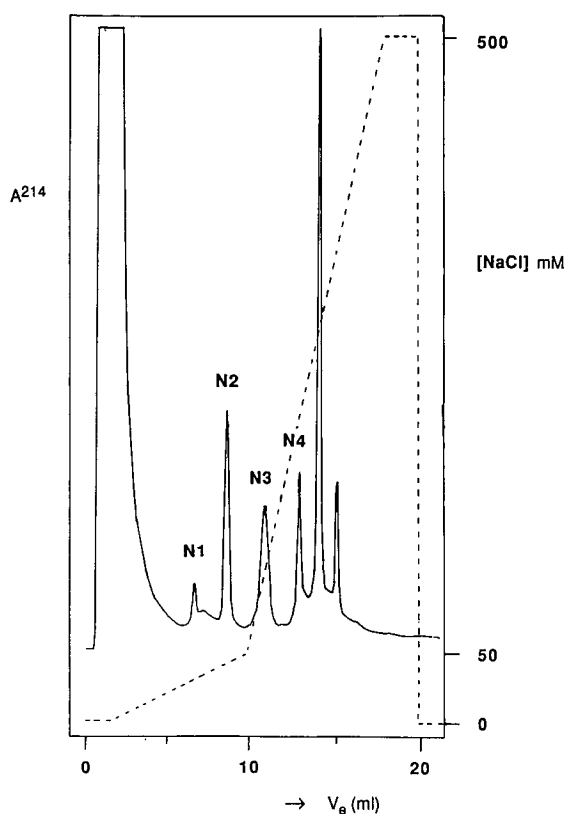


Fig. 3. Fractionation pattern at 214 nm of the carbohydrate-containing Bio-Gel P-100 fraction, derived from PNGase-F-treated K_2 tu-PA-I on a FPLC HR 5/5 Mono Q column. The column was first eluted with 2 ml H_2O , followed by a linear gradient (---) of 0–50 mM NaCl in 8 ml H_2O , and finally by a steeper gradient of 50–500 mM NaCl in 8 ml H_2O at a flow rate of 1 ml/min. The fractions were collected as indicated.

Liberation of the N-linked carbohydrate chains

The N-linked carbohydrate chains were released enzymically from the glycoprotein with PNGase-F [28]. Briefly, a solution of 46 mg K_2 tu-PA-I in 17 ml 25 mM sodium acetate pH 5.0, diluted to 23.3 ml, containing 30 mM Hepes, 50 mM EDTA, 1% (by vol.) 2-mercaptoethanol, and 1% (mass/vol.) SDS, and adjusted to pH 7.0 with 2 M NaOH was heated for 5 min at $95\text{--}100^\circ\text{C}$. Nonionic detergent Nonidet P-40 was added to the cooled solution to a final concentration of 1% (mass/vol.), and the mixture was incubated with 25 U PNGase-F for 4 h at ambient temperature. After the addition of a fresh aliquot of 25 U PNGase-F, the incubation was continued for 16 h. SDS/PAGE on a 12.5% slab gel (2.6% cross-linking) [29] and Coomassie brilliant blue staining was used to check the de-N-glycosylation.

The K_2 tu-PA-II, -III, and -IV batches (each 25 mg in 5 ml buffer as mentioned above) were mixed with 2.12 ml 0.2 M Tris, containing 0.2 M EDTA, 3.0% (by vol.) 2-mercaptoethanol, and 3.1% (mass/vol.) SDS, and adjusted to pH 7.4 with concentrated HCl. The B chain (5 mg) was dissolved in 1.76 ml 50 mM Tris, pH 7.4, containing 50 mM EDTA, 1.0% (by vol.) 2-mercaptoethanol, and 1.0% (mass/vol.) SDS, and the A chain (2 mg) in 6 ml 50 mM Tris, pH 7.4, containing 50 mM EDTA, 1.5% (by vol.) 2-mercaptoethanol, and 1.6% (mass/vol.) SDS. After heating for 5 min at $95\text{--}100^\circ\text{C}$, 710 μl 10% (mass/vol.) Nonidet P-40 was added to the K_2 tu-PA-II, -III, and -IV batches, 950 μl to the A chain and 185 μl

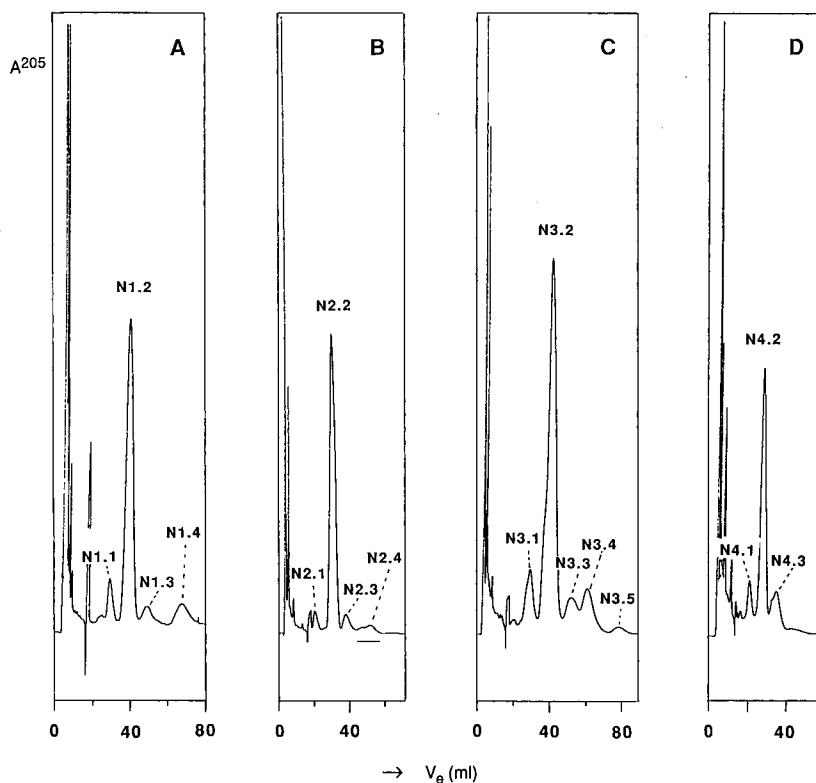


Fig. 4. Fractionation patterns at 205 nm of the Mono Q fractions N1–N4 from K_2 tu-PA-I on a 10- μ m Lichrosorb-NH₂ column (0.46 \times 25 cm). The column was eluted isocratically with a mixture of 30 mM K_2HPO_4/KH_2PO_4 pH 7.0/acetonitrile (36 : 64, by vol.) at a flow rate of 120 ml/h at ambient temperature. (A) FPLC Mono Q fraction N1; (B) fraction N2; (C) fraction N3; (D) fraction N4.

to the B chain. The K_2 tu-PA-II, -III, and -IV samples were digested twice with 12.4 U PNGase-F, in each case introduced at $t = 0$ and $t = 16$ h. In a similar way the A chain was treated twice with 2.0 U PNGase-F and the B chain twice with 2.5 U PNGase-F. The complete de-N-glycosylation was checked by SDS/PAGE and confirmed by using the 'Glycan detection kit' method B (Boehringer), and staining the nitrocellulose blotted paper for 3 h.

Isolation of the liberated N-linked carbohydrate chains

The released carbohydrate chains of K_2 tu-PA-I were collected and fractionated as described [24, 28]. The carbohydrate-positive Bio-Gel P-100 fractions of the K_2 tu-PA-II, -III and -IV, and of the A- and B-chain digests were lyophilised, and each transferred to a column (2.5 \times 45 cm) of Bio-Gel P-6 (200–400 mesh, Bio-Rad), eluted with 50 mM NH_4HCO_3 pH 7, at a flow rate of 16 ml/h and monitored at 206 nm. The carbohydrate-positive fractions (resorcinol/sulfuric acid and 300-MHz ¹H-NMR spectroscopy) were pooled, lyophilised, desalted, and fractionated [24, 28].

The molar ratio of oligosaccharides was determined on basis of absorbance at 205 nm (HPLC on Lichrosorb-NH₂) and at 214 nm (FPLC on Mono Q) [28].

Isolation of Neu5Ac α 2-3Gal β 1-4Glc from rat urine

Rat urine (900 ml), a known source of 9-O-acetylated sialyllactose [30], was concentrated by lyophilisation to 180 ml, and then applied to a column (3.5 \times 110 cm) of Bio-Gel P-6 (200–400 mesh) in three runs, using 0.1 M ammonia/acetic acid pH 5.5, as eluent at a flow rate of 48 ml/h. The effluent

was monitored at 206 nm. Aliquots of 20 μ l from the 12-ml fractions were stained for carbohydrate with resorcinol/sulfuric acid. TLC on silica gel (0.1 mm) coated on plastic sheet (Merck) was carried out to trace the presence of sialyloligosaccharides in carbohydrate-positive fractions, using ethanol/1-butanol/pyridine/water/acetic acid (100:10:10:30:3, by vol.) as solvent system. Neu5Ac α 2-3Gal β 1-4Glc and Neu5Ac α 2-6Gal β 1-4Glc from bovine colostrum (Sigma), and Neu5Ac were used as reference compounds. The sialic-acid-containing compounds were visualised with the orcinol/Fe³⁺/HCl (Bial) reagent [31]. Sialyloligosaccharide-containing fractions were combined, and the volume of the pool was adjusted to 250 ml with ammonia/acetic acid pH 5.5. Then, the solution was rinsed through a column (2.6 \times 43 cm) of AG 50W-X4 (Na⁺ form, 200–400 mesh, Bio-Rad), followed by 300 ml bidistilled water at a flow rate of 75 ml/h. The residue of the lyophilised eluent was dissolved in 30 ml water, and desalted on a column (2.6 \times 48 cm) of Bio-Gel P-2 (200–400 mesh) in two runs, using water as eluent, at a flow rate of 35 ml/h and detection at 206 nm. The void volume was collected, lyophilised, and the residue was dissolved in 2.5 ml water. Fractionation according to charge was carried out on a Q-Sepharose FF anion-exchange column (1.6 \times 7 cm), using a Pharmacia FPLC system. The elution was performed with 16 ml water, followed by a linear gradient of 0–75 mM NaCl in 84 ml water, and then a steeper gradient of 75–500 mM NaCl in 40 ml water, at a flow rate of 240 ml/h. The effluent was monitored at 214 nm, and the fraction containing sialyloligosaccharides (TLC analysis, Bial staining), eluting at the position of sialyllactose, was collected, lyophilised, desalted on a Bio-Gel P-2 column (2.6 \times 48 cm), and lyophilised again.

Table 1. (continued)

Reporter group	Residue	Chemical shift in						
		N1.2	N2.1	N2.2	N2.3A	N2.3B	N2.4A	N2.4B
		ppm						
	Fuc β	1.220	1.222	1.222	1.222	1.222	1.222	1.222

^a Values given with only two decimals because of spectral overlap.

^b Signal stemming from one NAc group.

^c Signal stemming from two NAc groups.

For the detection of *O*-acetylated sialyloligosaccharides in the Q-Sepharose fraction, 2D-TLC analysis with intermediate saponification of ester linkages was applied. Both dimensions were developed in the aforementioned solvent system. Prior to development of the second dimension, the plate was incubated for 16 h at ambient temperature in a chamber over a solution of 5 M NH₄OH.

Subfractionation of the Q-Sepharose fraction was carried out on a 10- μ m Partisil 10 SAX column (0.46 \times 25 cm, Whatman) using the Kratos HPLC system and detection at 205 nm [32]. Desalted HPLC fractions were investigated by 300-MHz ¹H-NMR spectroscopy. On guidance of the singlet at δ 2.140, corresponding with a 9-*O*-acetylated sialic acid [33], fractions were pooled and lyophilised. The residue was dissolved in 200 μ l water and further subfractionated on a 5- μ m Lichrospher 100-NH₂ HPLC column (0.46 \times 25 cm, Chrompack). Elutions were performed with a mixture of 30 mM K₂HPO₄/KH₂PO₄ pH 7.0 and acetonitrile (35 : 65, by vol.) at a flow rate of 90 ml/h and monitoring the effluent at 205 nm. HPLC fractions were desalted and analysed by 500-MHz ¹H-NMR spectroscopy.

Monosaccharide analysis

Monosaccharide analysis was carried out by GLC on a capillary SE-30 WCOT fused silica column (25 m \times 0.32 mm, Chrompack) using a Varian Aerograph 3700 gas chromatograph. The trimethylsilylated (methyl ester) methyl glycosides were prepared by methanolysis (1.0 M methanolic HCl, 24 h, 85°C), *N*-acetylation, and trimethylsilylation [34].

Sialic acid analysis

The analysis of sialic acids was carried out essentially as described [35]. An amount of 1 mg K₂tu-PA-I in 200 μ l 2 M acetic acid or 4 μ l (2% by vol.) from HPLC fractions in 40 μ l 2 M acetic acid were heated for 3 h at 80°C. Neu5Ac, Neu5Gc, and Neu5,9Ac₂ α -2-6Gal β 1-4GlcNAc were taken through the procedure as standards. HPLC analysis was carried out on a Chromspher C₁₈ reverse-phase column (25 \times 0.46 cm; Chrompack) as described [24].

300-MHz, 500-MHz, and 600-MHz ¹H-NMR spectroscopy

Prior to ¹H-NMR spectroscopy of oligosaccharide samples in ²H₂O, they were repeatedly treated with 99.8% ²H₂O (MSD Isotopes) at p²H 7 with intermediate lyophilisation, finally using 99.96% ²H₂O [36]. Prior to ¹H-NMR spectroscopy of Neu5,9Ac₂ α -2-6Gal β 1-4GlcNAc in ¹H₂O, the native sample was dissolved in 450 μ l 20 mM K₂HPO₄, containing 92.5% (by vol.) ¹H₂O, 7.5% (by vol.) ²H₂O, and

0.02% (mass/vol.) sodium azide; the pH was adjusted to 5.7 with 0.5 M HCl [37].

300-MHz, 500-MHz, and 600-MHz one-dimensional (1D) and two-dimensional (2D) ¹H-NMR spectra were recorded on spectrometers Bruker AC-300 (Department of Organic Chemistry, Utrecht University), Bruker AM(X)-500 (Bijvoet Center, Department of NMR spectroscopy, Utrecht University), and Bruker AM-600 (NSR Center, SON NMR facility, University of Nijmegen, The Netherlands), respectively, at probe temperatures of 300 K, unless indicated otherwise. Chemical shifts are expressed in ppm relative to internal acetone (δ 2.225 in ²H₂O at 300 K [36]). 500-MHz 1D spectra were recorded as described [38].

The 300-MHz 2D-COSY spectra of Neu5,9Ac₂ α -2-3Gal β 1-4Glc and Neu5,9Ac₂ α -2-6Gal β 1-4GlcNAc in ²H₂O at 298 K were obtained as described [39, 40]. The spectral width was 1800 Hz for Neu5,9Ac₂ α -2-3Gal β 1-4Glc and 1500 Hz for Neu5,9Ac₂ α -2-6Gal β 1-4GlcNAc, respectively, in each dimension. Data matrices of 360 \times 2048 and 512 \times 2048 points were recorded for Neu5,9Ac₂ α -2-3Gal β 1-4Glc and Neu5,9Ac₂ α -2-6Gal β 1-4GlcNAc, respectively.

The 500-MHz 2D-HOHAHA spectrum of Neu5,9Ac₂ α -2-3Gal β 1-4Glc in ²H₂O was recorded [41, 42] using a MLEV-17 mixing sequence of 120 ms with a spin-lock field strength corresponding to a 90° ¹H pulse width of 28.3 μ s. A 307 \times 2048 data matrix, presenting a spectral width of 2400 Hz in each dimension, was recorded. For the 500-MHz 2D-HOHAHA spectrum of Neu5,9Ac₂ α -2-6Gal β 1-4GlcNAc in ¹H₂O, a MLEV-17 mixing sequence of 100 ms with a spin-lock field strength corresponding to a 90° ¹H pulse width of 29.2 μ s was used. The spectral width was 3700 Hz in each dimension, and a number of 512 \times 2048 data points were recorded.

The 600-MHz 2D-HOHAHA spectrum of Neu5,9Ac₂ α -2-6Gal β 1-4GlcNAc in ²H₂O was recorded at 280 K, using a MLEV-17 mixing sequence of 120 ms with a spin-lock field strength corresponding to a 90° ¹H pulse width of 25.9 μ s. The spectral width was 3700 Hz in each dimension and 512 \times 2048 data points were recorded.

The 600-MHz 2D-ROESY spectra of Neu5,9Ac₂ α -2-6Gal β 1-4GlcNAc at 280 K in ¹H₂O and in ²H₂O were obtained as described [43], using a spin-lock mixing pulse of 200 ms at a field strength corresponding to a 90° ¹H pulse width of 115 μ s. The spectral width was 3521 Hz in each dimension in the case of ²H₂O as solvent, and 4807 Hz with ¹H₂O as solvent. In both cases, the carrier frequency was placed on the 'water-line' at 5.0 ppm.

In the case of the 2D NMR experiments, the water signal was suppressed by presaturation. Phase-sensitive handling of the data in the ω_1 dimension became possible by the time-proportional phase-increment method [39]. The time domain

Table 2. ¹H-chemical shifts of structural-reporter-group protons of constituent monosaccharides of the trisialylated N-linked oligosaccharides derived from K₂tu-PA. Chemical shifts are given relative to internal acetone (δ 2.225) in ²H₂O at 300 K and at p²H 7 [36]. Compounds are represented by short-hand symbolic notation: (□), L-Fuc; (■), D-Gal; (●), D-GlcNAc; (◆), D-Man; (△), D-Neu5Ac α (2-3); (△), D-Neu5Gc α (2-3). For numbering of the monosaccharide residues, see text. n. d., not determined. α and β stand for the anomeric configuration of GlcNAc-1.

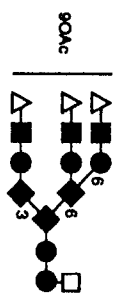
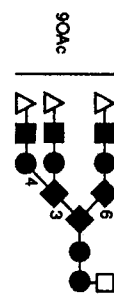
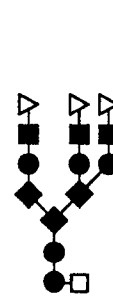
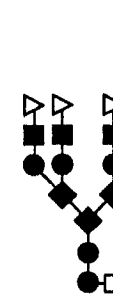
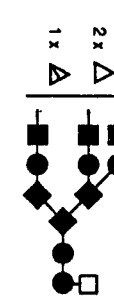
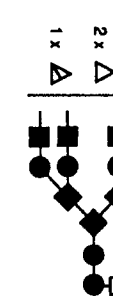
Reporter group	Residue	Chemical shift in					
		N3.1A	N3.1B	N3.2A	N3.2B	N3.3A	N3.3B
							
		ppm					
H-1	GlcNAc-1 α	5.182	5.182	5.182	5.182	5.181	5.181
	GlcNAc-1 β	4.690	4.690	4.690	4.690	4.690	4.690
	GlcNAc-2 α	4.663	4.663	4.662	4.662	4.661	4.661
	GlcNAc-2 β	4.663	4.663	4.664	4.664	4.663	4.663
	Man-4	5.118	5.114	5.122	5.113	5.122	5.114
	Man-4'	4.870	4.902	4.871	4.903	4.870	4.904
	GlcNAc-5	4.577	4.559	4.577	4.560	4.578	4.561
	GlcNAc-5'	4.587	4.577	4.587	4.577	4.588	4.578
	Gal-6	4.544	4.544	4.544	4.544	4.545	4.545
	Gal-6'	4.544	4.544	4.544	4.544	4.545	4.545
	GlcNAc-7	—	4.544	—	4.544	—	4.545
	GlcNAc-7'	4.544	—	4.544	—	4.545	—
	Gal-8	—	4.544	—	4.544	—	4.545
	Gal-8'	4.559	—	4.560	—	4.561	—
Fuc α	4.899	4.899	4.899	4.899	4.899	4.899	
Fuc β	4.906	4.906	4.907	4.907	4.908	4.908	
H-2	Man-3	4.250	4.209	4.250	4.210	4.250	4.213
	Man-4	4.194	4.209	4.197	4.210	4.199	4.213
	Man-4'	4.089	4.106	4.090	4.105	4.090	4.106
H-3	Gal-6	4.115	4.115	4.116	4.116	4.115	4.115
	Gal-6'	4.115	4.115	4.116	4.116	4.115	4.115
	Gal-8	—	4.115	—	4.116	—	4.115
	Gal-8'	4.115	—	4.116	—	4.115	—
H-3a	Neu5Ac	1.802 ^a	1.802 ^a	1.802 ^a	1.802 ^a	1.803 ^b	1.803 ^b
	Neu5Gc	—	—	—	—	1.821 ^c	1.821 ^c
H-3e	Neu5Ac	2.756 ^a	2.756 ^a	2.757 ^a	2.757 ^a	2.757 ^b	2.757 ^b
	Neu5Gc	—	—	—	—	2.776 ^c	2.776 ^c
H-5	Fuc α	4.100	4.100	4.102	4.102	4.097	4.097
	Fuc β	4.132	4.132	4.133	4.133	4.132	4.132
H-6	Man-4'	4.210	n. d.	4.210	n. d.	4.211	n. d.
H-8	Neu5,9Ac ₂	4.11 ^d	4.11 ^d	—	—	—	—
H-9	Neu5,9Ac ₂	4.417	4.417	—	—	—	—
H-9'	Neu5,9Ac ₂	4.191	4.191	—	—	—	—
NAc	GlcNAc-1	2.038	2.038	2.038	2.038	2.039	2.039
	GlcNAc-2 α	2.094	2.094	2.094	2.094	2.094	2.094
	GlcNAc-2 β	2.094	2.094	2.092	2.092	2.094	2.094
	GlcNAc-5	2.051	2.043	2.051	2.043	2.052	2.042
	GlcNAc-5'	2.038	2.043	2.038	2.043	2.039	2.042
	GlcNAc-7	—	2.073	—	2.073	—	2.075
	GlcNAc-7'	2.038	—	2.038	—	2.039	—
	Neu5Ac	2.031 ^e	2.031 ^e	2.031 ^f	2.031 ^f	2.031 ^e	2.031 ^e
	Neu5,9Ac ₂	2.038 ^g	2.038 ^g	—	—	—	—
	NGc	Neu5Gc	—	—	—	—	4.121
OAc	Neu5,9Ac ₂	2.142	2.142	—	—	—	—

Table 2. (continued)

Reporter group	Residue	Chemical shift in					
		N3.1A	N3.1B	N3.2A	N3.2B	N3.3A	N3.3B
		ppm					
CH ₃	Fuc _α	1.211	1.211	1.211	1.211	1.211	1.211
	Fuc _β	1.222	1.222	1.223	1.223	1.223	1.223

^a Signal stemming from three protons.

^b Signal stemming from two protons.

^c Signal stemming from one proton.

^d Values given with only two decimals because of spectral overlap.

^e Signal stemming from two NAc groups.

^f Signal stemming from three NAc groups.

^g Signal stemming from one NAc group.

data of the COSY, HOHAHA, and ROESY experiments were zero-filled to 1024 × 2048 data matrices prior to multiplication with a phase-shifted squared-bell and a phase-sensitive Fourier transformation.

RESULTS

Isolation and structure determination of the N-linked chains of K₂tu-PA-I

Monosaccharide analysis of recombinant K₂tu-PA-I revealed a carbohydrate content of 6% (by mass) and the presence of Fuc, Gal, Man, GlcNAc, and Neu5Ac in the molar ratio of 1.0 : 2.6 : 3.0 : 4.2 : 2.5 (mean values of two runs; the value of GlcNAc has been corrected for the relatively stable GlcNAc-Asn linkage [34]). Sialic acid analysis of native K₂tu-PA-I revealed the occurrence of Neu5Ac as major component (94%), and Neu5Gc (3%) and Neu5,9Ac₂ (3%) as minor components. The absence of GalNAc implies that neither mucin-type carbohydrate chains nor N-linked chains containing GalNAcβ1-4GlcNAc elements occur. As evidenced by SDS/PAGE (Fig. 2, lane 2), the K₂tu-PA-I preparation shows bands at apparently (a) 40–42 kDa (K₂tu-PA; glycosylated B chain with non-glycosylated A chain, lower part; glycosylated B chain with glycosylated A chain, upper part); (b) 33 kDa (glycosylated B chain of K₂tu-PA); (c) 17 kDa (glycosylated A chain of K₂tu-PA); and (d) 13 kDa (non-glycosylated A chain of K₂tu-PA). The K₂tu-PA-I preparation exists partly in a two-chain form, which gives rise to the separate A and B chains under reducing conditions. A PNGase-F time course experiment monitored by SDS/PAGE shows the presence of one N-linked oligosaccharide attachment site on the protease domain of K₂tu-PA (B chain) and on the A chain, which is occupied for about 10%. A complete PNGase-F digestion shows only SDS/PAGE bands (Fig. 2, lane 8) at apparently (a) 36 kDa (de-N-glycosylated K₂tu-PA; A + B chain); (b) 30 kDa (de-N-glycosylated B chain of K₂tu-PA); and (c) 13 kDa (de-N- and non-glycosylated A chain of K₂tu-PA).

FPLC anion-exchange chromatography of the Bio-Gel P-100 oligosaccharide fraction on Mono Q gave rise to four carbohydrate-positive peaks, denoted N1–N4 (Fig. 3). Fractions N1, N2, N3, and N4 have the same retention volumes as reference monosialylated diantennary, disialylated diantennary, trisialylated tri-/tri'-antennary, and tetrasialylated tetraantennary oligosaccharides, respectively [44]. The remaining peaks eluting before N1 and after N4 do not corre-

spond with carbohydrate material (resorcinol/sulfuric acid assay).

HPLC on Lichrosorb-NH₂ of Mono Q fraction N1 gave rise to four subfractions, denoted N1.1–N1.4 (Fig. 4 A). Similarly, Mono Q fraction N2 yielded four subfractions N2.1–N2.4 (Fig. 4 B), whereas Mono Q fraction N3 has been subfractionated into N3.1–N3.5 (Fig. 4 C), and Mono Q fraction N4 into N4.1–N4.3 (Fig. 4 D). All HPLC subfractions were analysed by 500-MHz ¹H-NMR spectroscopy. Relevant ¹H-NMR data are compiled in Tables 1–3, and compounds will be discussed in order of increasing complexity. The amount of material in fractions N1.1, N1.3, N1.4, and N3.5 was too low for a reliable structure determination by ¹H-NMR spectroscopy.

All compounds have the α(1-6)-fucosylated N₂N'-diacetylchitobiose unit in common, as is evident from the ¹H-NMR data [38]. The Neu5Ac residues are exclusively present in α(2-3)-linkage at Gal (NAc, δ 2.031–2.032; H-3e, δ 2.755–2.759; H-3a, δ 1.796–1.803). Furthermore, the existence of N-glycolyl- and 9-O-acetyl-groups in the carbohydrate chains derived from K₂tu-PA-I was checked by sialic acid analysis of relevant HPLC fractions.

The ¹H-NMR spectrum of fraction N1.2 indicates a fucosylated, α(2-3)-monosialylated (Neu5Ac) diantennary oligosaccharide (cf. compound C-Q1-1 in [45]; see Table 4), and that of fraction N2.2 a fucosylated, α(2-3)-disialylated (Neu5Ac) diantennary oligosaccharide (cf. compound N2.5 in [38]; see Table 4). The ¹H-NMR spectrum of fraction N2.3 shows the presence of two fucosylated, α(2-3)-disialylated diantennary oligosaccharide analogs of N2.2 in about equal amounts (Fig. 5 A). They differ from N2.2 by the replacement of a Neu5Ac by a Neu5Gc residue at either the Manα(1-6) branch (N2.3A) or the Manα(1-3) branch (N2.3B) [24] (see Table 4).

¹H-NMR analysis of fraction N3.2 demonstrates the occurrence of a minor component (25%): fucosylated, α(2-3)-trisialylated (Neu5Ac) triantennary oligosaccharide N3.2B (cf. compound N3.2A in [44]; see Table 4); and a major component (75%): fucosylated, α(2-3)-trisialylated (Neu5Ac) tri'-antennary oligosaccharide N3.2A (cf. compound N3.3 in [44]; see Table 4). The position of Man-4' H-2 at δ 4.090 was recently established by 2D-ROESY, and turned out to be specific for tri'- [46] and tetraantennary structures (unpublished results). Also the Man-4' H-6 signal at δ 4.210 can be used as an extra structural-reporter-group signal for tri'- and tetraantennary structures, as recently discussed [38].

Table 3. ¹H-chemical shifts of structural-reporter-group protons of constituent monosaccharides of the tetrasialylated N-linked oligosaccharides derived from K₂tu-PA. Chemical shifts are given relative to internal acetone (δ 2.225) in ²H₂O at 300 K and at p²H 7 [36]. Compounds are represented by short-hand symbolic notation: (□), L-Fuc; (■), D-Gal; (●), D-GlcNAc; (◆), D-Man; (△), D-Neu5Ac α (2-3); (Δ), D-Neu5Gc α (2-3). For numbering of the monosaccharide residues, see text. n. d., not determined. α and β stand for the anomeric configuration of GlcNAc-1.

Reporter group	Residue	Chemical shift in		
		N4.1	N4.2	N4.3
		ppm		
H-1	GlcNAc-1 α	5.182	5.184	5.183
	GlcNAc-1 β	4.690	4.689	n. d.
	GlcNAc-2 α	4.662	4.661	n. d.
	GlcNAc-2 β	4.662	4.664	n. d.
	Man-4	5.131	5.131	5.131
	Man-4'	4.855	4.858	4.856
	GlcNAc-5	4.560	4.560	4.560
	GlcNAc-5'	4.592	4.593	4.593
	Gal-6	4.545	4.543	4.544
	Gal-6'	4.545	4.543	4.544
	GlcNAc-7	4.545	4.543	4.544
	GlcNAc-7'	4.545	4.543	4.544
	Gal-8	4.545	4.543	4.544
	Gal-8'	4.560	4.560	4.560
	Fuc α	4.902	4.902	4.901
	Fuc β	4.908	4.908	4.908
H-2	Man-3	4.207	4.205	4.204
	Man-4	4.219	4.219	4.218
	Man-4'	4.090	4.091	4.092
H-3	Gal-6/6'	4.117	4.117	4.116
	Gal-8/8'	4.117	4.117	4.116
H-3a	Neu5Ac	1.804 ^a	1.804 ^a	1.803 ^b
	Neu5Gc	—	—	1.821
H-3e	Neu5Ac	2.757 ^a	2.757 ^a	2.757 ^b
	Neu5Gc	—	—	2.776
H-5	Fuc α	4.10 ^c	4.10 ^c	4.10 ^c
	Fuc β	4.13 ^c	4.13 ^c	4.13 ^c
H-6	Man-4'	4.212	4.212	4.212
H-8	Neu5,9Ac ₂	4.11 ^c	—	—
H-9	Neu5,9Ac ₂	4.420	—	—
H-9'	Neu5,9Ac ₂	4.195	—	—
NAc	GlcNAc-1	2.038	2.039	2.038
	GlcNAc-2 α	2.094	2.094	2.093
	GlcNAc-2 β	2.094	2.091	2.093
	GlcNAc-5	2.047	2.048	2.048
	GlcNAc-5'	2.038	2.039	2.038
	GlcNAc-7	2.075	2.075	2.075
	GlcNAc-7'	2.038	2.039	2.038
	Neu5Ac	2.031 ^d	2.031 ^e	2.031 ^d
	Neu5,9Ac ₂	2.038 ^f	—	—
NGc	Neu5Gc	—	—	4.122
OAc	Neu5,9Ac ₂	2.143	—	—

Table 3. (continued)

Reporter group	Residue	Chemical shift in		
		N4.1	N4.2	N4.3
		ppm		
CH ₃	Fuc α	1.211	1.212	1.211
	Fuc β	1.223	1.223	1.223

^a Signal stemming from four protons.

^b Signal stemming from three protons.

^c Values given with only two decimals because of spectral overlap.

^d Signal stemming from three NAc groups.

^e Signal stemming from four NAc groups.

^f Signal stemming from one NAc group.

The ¹H-NMR spectrum of N2.4 showed the presence of a mixture of fucosylated, α (2-3)-disialylated (Neu5Ac) tri- (N2.4B) and tri'- (N2.4A) antennary carbohydrate chains (see Table 4). The presence of two sialic acid residues in both structures is proven by the relative intensities of the NAc, H-3a, and H-3e structural reporters of Neu5Ac, as compared to the ¹H-NMR spectrum of N3.2. The structural-reporter-group signals of the three antennae in N2.4B match those of the non-fucosylated analogue N2.3 in [44]. The tri'-antennary character of N2.4A is demonstrated by the H-1 signals of Man-4 and Man-4' at δ 5.125 and δ 4.868, respectively, the H-2 signals of Man-3, Man-4 and Man-4' at δ 4.250, δ 4.196, and δ 4.090, respectively, and the H-6 signal of Man-4' at δ 4.210. The position of the H-1 signal of Gal-8' at δ 4.481 indicates the presence of Gal-8' in terminal position, as in compound 11 in [36].

Comparison of the ¹H-NMR spectra of fractions N3.2 and N3.3 shows that also fraction N3.3 contains a mixture of fucosylated, α (2-3)-trisialylated tri- (N3.3B) and tri'- (N3.3A) antennary oligosaccharides. The same characteristic structural-reporter-group signals for the constituting Gal, GlcNAc, Man, and Fuc residues are found in comparable relative intensities as in N3.2. However, the region of the H-2 signal of α (1-6)-linked Man, the H-3 signal of Gal (3 \times), and the H-5 signal of Fuc of fraction N3.3, contains an additional singlet at δ 4.121, typical for the NGc methylene signal of Neu5Gc, as already discussed for N2.3A and N2.3B [24]. Furthermore, the NAc methyl singlet of Neu5Ac is reduced to about 70% relative to the Neu5Ac NAc signal in N3.2. Additional signals of H-3e and H-3a at δ 2.776 and δ 1.821, respectively, are observed, apart from the presence of the Neu5Ac H-3e and H-3a signals at δ 2.757 and δ 1.803, respectively, reflecting the occurrence of one Neu5Gc residue and two Neu5Ac residues. Based on these data, it can be concluded that N3.3 contains the components N3.3A and N3.3B (see Table 4), wherein the position of the sialic acids could not be specified.

The ¹H-NMR spectrum of N4.2 shows a fucosylated, α (2-3)-tetrasialylated (Neu5Ac) tetraantennary carbohydrate chain (cf. compound N4.2B in [44]; see Table 4), and that of N4.3 a modification of N4.2, in which one of the Neu5Ac residues has been replaced by a Neu5Gc residue (cf. compound A4.5 in [24]; see Table 4).

The ¹H-NMR spectrum of N2.1 (Fig. 5 B) resembles that of N2.2, and N2.1 could be identified as a fucosylated, α (2-3)-disialylated diantennary carbohydrate chain, with one of the Neu5Ac residues occurring as Neu5,9Ac₂ (see Table 4).

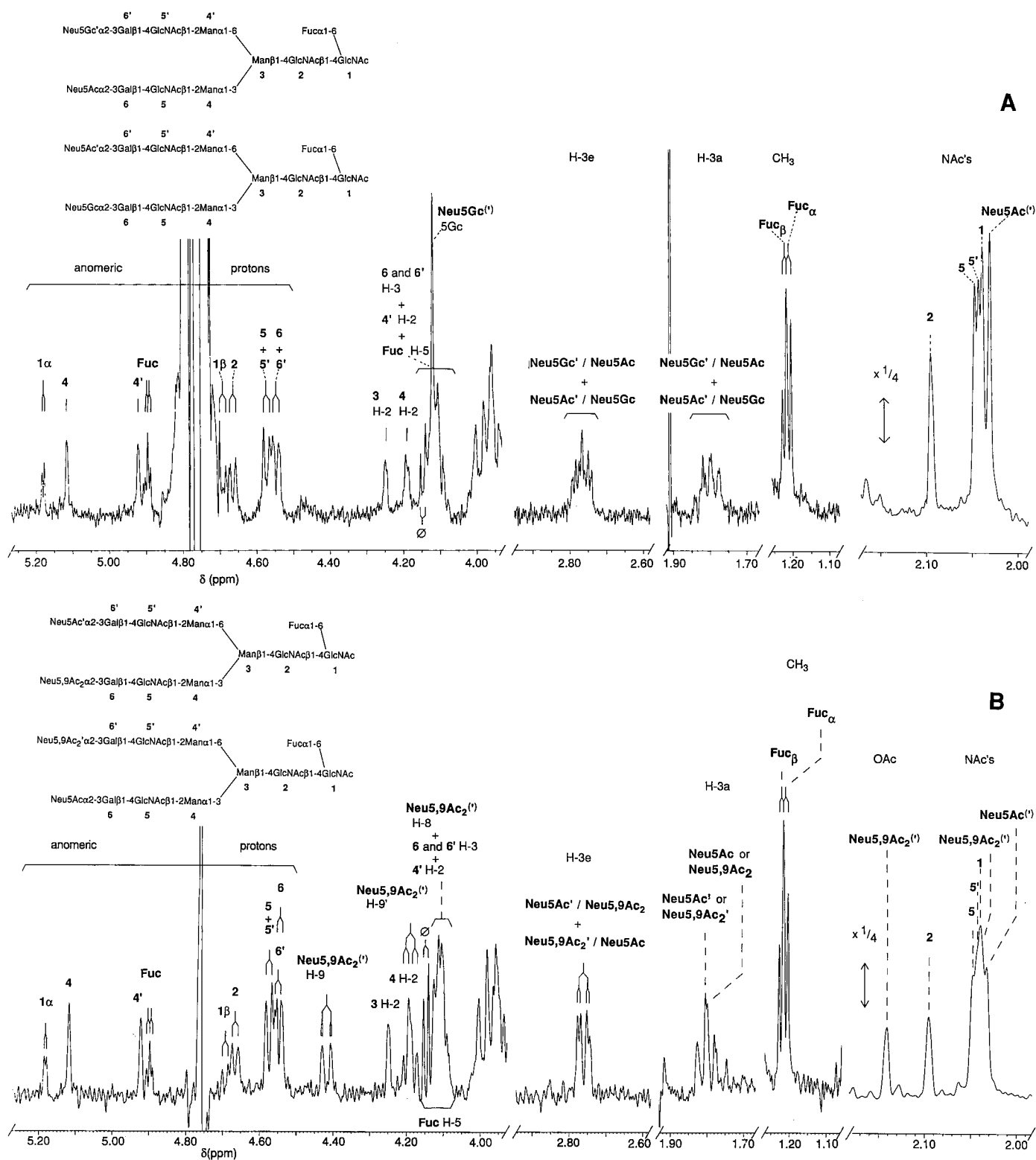


Fig. 5. Structural-reporter-group-signal regions of the resolution-enhanced 500-MHz $^1\text{H-NMR}$ spectra at 300 K of (A) mono-*N*-glycolylated, mono-*N*-acetylated (N2.3) and (B) mono-9-*O*-acetylated-*N*-acetylated, mono-*N*-acetylated (N2.1) α (2-3)-disialylated, α (1-6)-fucosylated diantennary oligosaccharide.

The $^1\text{H-NMR}$ spectrum of N4.1 resembles that of N4.2 so that N4.1 could be identified as a fucosylated, α (2-3)-tetrasialylated tetraantennary carbohydrate chain, in which Neu5Ac and Neu5,9Ac $_2$ residues occur (see Table 4). One out of four Neu5Ac residues is 9-*O*-acetylated, as is evident

from the *O*-acetyl methyl signal at δ 2.143 with an intensity comparable to that of the *N*-acetyl methyl signal of GlcNAc-2. In addition, the intensity of the *N*-acetyl methyl signal at δ 2.031 is decreased compared to that in N4.2, due to a downfield shift of one *N*-acetyl methyl signal to δ 2.038. The

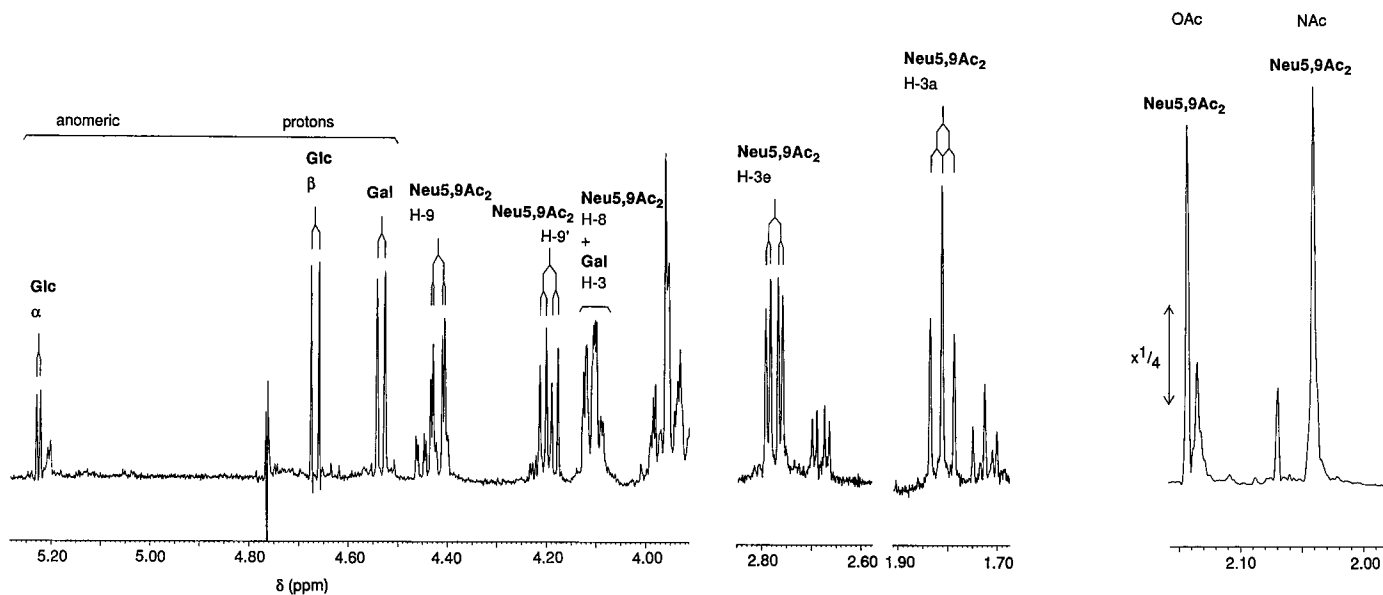
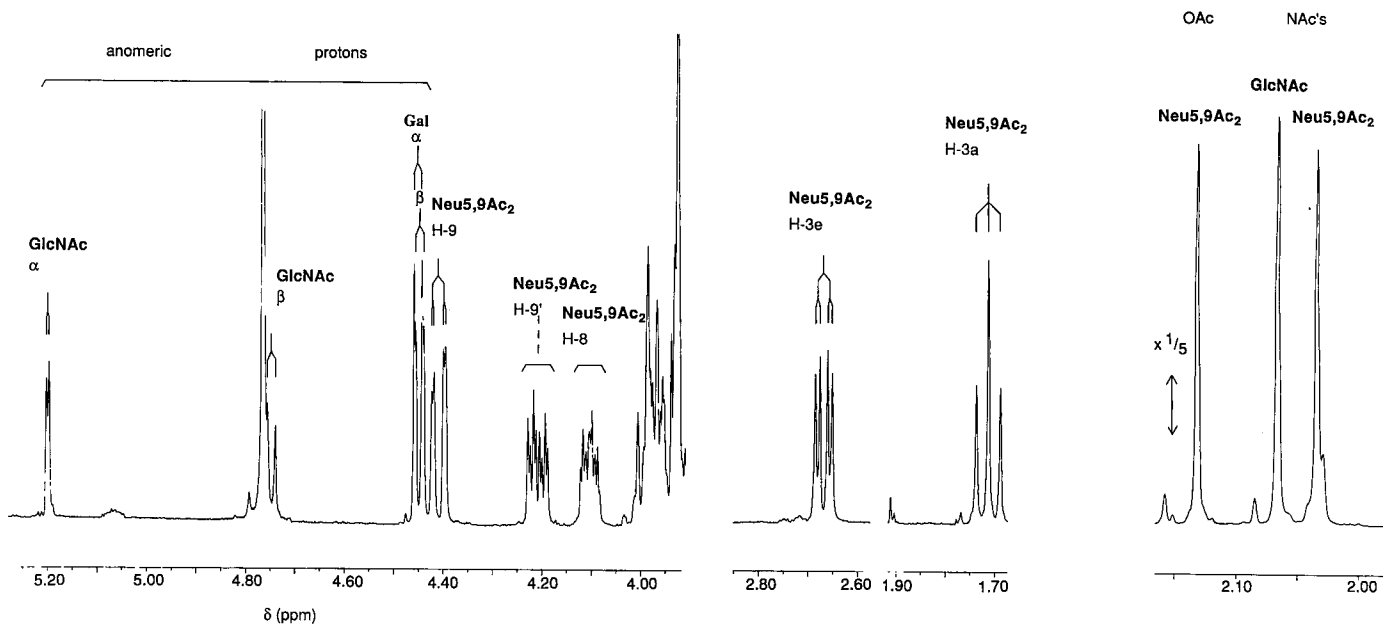
Neu5,9Ac₂α2-3Galβ1-4GlcNeu5,9Ac₂α2-6Galβ1-4GlcNAc

Fig. 6. Structural-reporter-group-signal regions of the resolution-enhanced 500-MHz ¹H-NMR spectra at 300 K of (A) Neu5,9Ac₂-¹³C-Lac, contaminated with Neu5,9Ac₂^{VI}LacNAc and (B) Neu5,9Ac₂^{VI}LacNAc.

9-*O*-acetylation is further reflected by H-9 and H-9' signals at δ 4.420 and δ 4.195, respectively, and H-8 at δ 4.11.

Profiling studies on the N-linked chains of K₂tu-PA-II, -III, and -IV batches and the A and B chain of K₂tu-PA-IV

To obtain information about the mixture of carbohydrate chains of different K₂tu-PA batches, and the mixture of carbohydrate chains present in the A chain (Asn12) and B

chain (Asn247) of K₂tu-PA, profiling studies were performed. For this purpose, the cleavage and fractionation procedure as discussed above was followed. The N-linked carbohydrate chains were released, and the completeness of the de-N-glycosylation was demonstrated by SDS/PAGE in combination with the glycan detection procedure. After Bio-Gel P-100 gel filtration, the carbohydrate-positive fraction, as verified by 300-MHz ¹H-NMR spectroscopy, was further purified on Bio-Gel P-6, desalted on Bio-Gel P-2, and fractionated on Mono Q. For K₂tu-PA-II, -III, and -IV, and the B

Table 5. ¹H-chemical shifts of structural-reporter-group protons of constituent monosaccharides of Neu5,9Ac₂α2-3Galβ1-4Glc, isolated from female Wistar rat urine, and Neu5,9Ac₂α2-6Galβ1-4GlcNAc, together with those for reference compound Neu5Aca2-3Galβ1-4Glc [48], Neu5Aca2-6Galβ1-4GlcNAc [49], Neu5Aca2-3Galβ1-4GlcNAcβ(1-N)Asn [47] and Neu5Aca2-6Galβ1-4GlcNAcβ(1-N)Asn [47]. Chemical shifts are given relative to internal acetone (δ 2.225) in ²H₂O at 300 K (281 K for third and sixth compounds) and at p²H 7 [36]. Values for the fifth compound were taken from [49] and corrected relative to acetone at δ 2.225. Compounds are represented by short-hand symbolic notation: (Δ), Neu5Aca(2-3); (○), Neu5Aca(2-6); (◐), Neu5,9Ac₂α(2-3); (◑), Neu5,9Ac₂α(2-6); (■), Gal; (●), Glc; (●), GlcNAc. n. d., not determined. α and β stand for the anomeric configuration of reducing Glc or GlcNAc.

Residue	Protons	Chemical shift in					
		ppm					
Neu5Ac	H-3a	1.798	1.799	1.801	1.713	1.713	1.717
	H-3e	2.761	2.757	2.774	2.669	2.670	2.662
	H-4	3.689	n. d.	3.684	3.660	n. d.	3.639
	H-5	3.868	n. d.	3.854	3.830	n. d.	3.805
	H-6	3.671	n. d.	3.618	3.741	n. d.	3.694
	H-7	3.639	n. d.	3.593	3.610	n. d.	3.547
	H-8	4.114	n. d.	3.903	4.103	n. d.	3.889
	H-9	4.415	n. d.	3.867	4.410	n. d.	3.875
	H-9' _α	4.190	n. d.	3.633	4.211	n. d.	3.627
	H-9' _β	4.190	n. d.	3.633	4.207	n. d.	3.627
	NAc	2.036	2.030	2.028	2.034	2.028	2.028
	OAc	2.139	—	—	2.132	—	—
	NH	n. d.	n. d.	n. d.	8.04 ^a	n. d.	n. d.
	Gal	H-1 _α	4.529	4.530	—	4.451	4.452
H-1 _β		4.529	4.528	4.572	4.448	4.448	4.447
H-2		3.569	n. d.	3.582	3.553	n. d.	3.537
H-3 _α		4.108	4.114	—	3.680	n. d.	—
H-3 _β		4.108	4.110	4.128	3.680	n. d.	3.668
Glc/GlcNAc	H-4	3.941	3.959	3.957	3.940	n. d.	3.917
	H-1 _α	5.221	5.220	—	5.200	5.199	—
	H-1 _β	4.662	4.661	5.107	n. d.	4.759	5.134
	H-2 _α	3.579	n. d.	—	3.938	n. d.	—
	H-2 _β	3.284	3.281	3.895	3.75 ^a	n. d.	3.881
	NAc	—	—	2.014	2.067	2.065	2.042
	NH _α	—	—	n. d.	8.06 ^a	n. d.	n. d.
NH _β	—	—	n. d.	8.17 ^a	n. d.	n. d.	

^a Value determined from 2D ¹H NMR experiments at 280 K.

Table 6. Molar percentages of mono-, di-, tri-, and tetrasialylated oligosaccharides occurring in different batches of K₂tu-PA and in the glycopeptides obtained from K₂tu-PA-IV. Results are based on peak areas of Mono Q peaks and are corrected for the number of carbonyl groups of the components, as determined by HPLC on Lichrosorb-NH₂, contributing to the different peaks. n. d., not determined.

Batch number/peptide	Sialylation			
	mono	di	tri	tetra
	mol/100 mol			
K ₂ tu-PA-I	8	47	28	17
K ₂ tu-PA-II	4	54	31	11
K ₂ tu-PA-III	4.9 ± 0.7 ^a	52.8 ± 0.5 ^a	29.9 ± 0.9 ^a	12.3 ± 1.4 ^a
K ₂ tu-PA-IV	6	53	28	12
A chain (K ₂ tu-PA-IV)	18	61	7	14 ^b
B chain (K ₂ tu-PA-IV)	n. d.	54	33	13

^a Mean ± SD determined from three successive runs on Mono Q HR5/5.

^b The quantity of oligosaccharide in fraction N4 is overestimated, as indicated by HPLC analysis on Lichrosorb-NH₂, showing the presence of non-carbohydrate material.

chain of K₂tu-PA-IV similar Mono Q patterns for the N-linked oligosaccharides were obtained as shown for K₂tu-PA-I (Fig. 3), but the A chain of K₂tu-PA-IV gave rise to a different pattern. The amounts of mono-, di-, tri-, and tetrasialylated oligosaccharide per peak were quantified, and are listed in Table 6. The V₀ peak and the peaks eluting after the tetrasialylated tetraantennary oligosaccharide fraction do not contain carbohydrate material as tested by 300-MHz ¹H-NMR spectroscopy (i. e. acetyl region).

For the subfractionation of the Mono Q fractions derived from K₂tu-PA-II, -III, and -IV, and the A and B chain of K₂tu-PA-IV by HPLC, a Lichrosorb-NH₂ column was calibrated with the oligosaccharides derived from the K₂tu-PA-I batch and with a nonfucosylated disialylated diantennary oligosaccharide from recombinant human follitropin [44]. Major peaks of each K₂tu-PA batch were checked by 500-MHz ¹H-NMR spectroscopy. In Table 4 a compilation is presented of the carbohydrate structures and their relative amounts for the various K₂tu-PA batches. It was found qualitatively that the collection of the N-linked oligosaccharides of K₂tu-PA-I is identical to that of K₂tu-PA-II, -III, and -IV. However, the method used for the culturing and isolation of K₂tu-PA seems to give rise to subtle differences in relative quantities.

The glycosylation sites on the A (Asn12) and B chain (Asn247) show identical arrays of micro-heterogeneity. However, mono- and disialylated compounds have a higher relative abundance on the A chain than on the B chain as well as on native K₂tu-PA, whereas the reverse holds for the tri- and tetrasialylated compounds. The molar ratio tri-/tri'-antennary structures changes from 1 : 5.4 on the B chain to 1 : 1.5 on the A chain (Table 4).

DISCUSSION

In Table 4 a compilation is given of the structures and relative molar amounts of the carbohydrate chains occurring in K₂tu-PA samples. The sialic acid residues are present in non-reducing terminal positions, solely $\alpha(2-3)$ -linked to a penultimate β -Gal residue, in accordance with the suggested absence of β -Gal: $\alpha(2-6)$ -sialyltransferase activity in CHO cells [23]. However, recently indications for significant amounts of $\alpha(2-6)$ -linked sialic acid were reported for *N*-acetylglucosamine type of carbohydrate chains on Asn289 of recombinant human plasminogen expressed in CHO cells [50]. The use of PNGase-F to release the carbohydrate chains from K₂tu-PA made it possible to also pay attention to the authentic sialylation pattern of K₂tu-PA. The presence of Neu5Gc (3%) and the possible relevance of its appearance in recombinant-DNA glycoproteins of pharmaceutical interest expressed in CHO cells has already been discussed [24]. The presence of Neu5,9Ac₂ (3%) in the carbohydrate moiety of recombinant glycoproteins expressed in CHO cells has not been reported so far, and it implies the existence of an active *O*-acetyltransferase system (cf. [51, 52]). Because the occurrence of 9-*O*-acetylated *N*-acetylneuraminic acid in human tissue has been well established [51], no consequences of this feature of biotechnologically engineered glycosylated proteins like K₂tu-PA in pharmaceutical utilisation can be anticipated.

The sialylation of K₂tu-PA (2.5 : 1) is much higher than for recombinant t-PA (cf. 1.1 : 1 [42]) or a recombinant t-PA variant (Asn117 and Asn184 replaced by Gln117 and Gln184, respectively; cf. 1.7 : 1 [53]), both expressed in

CHO cells. Outer chain processing, including sialylation and fucosylation, reflects the glycosylation apparatus of the host cell. In this respect, clonal variations and cell culture conditions may have affected the $\alpha(2-3)$ -sialyltransferase activity. The N-linked carbohydrate chains of K₂tu-PA were completely $\alpha(1-6)$ -fucosylated at the innermost GlcNAc residue. The recombinant t-PA [45] and variant recombinant t-PA [53], expressed in CHO cells, are also almost fully fucosylated, whereas human colon fibroblast t-PA is fucosylated for 58% [8]. Other structural differences occur in the ratio of tri- and tri'-antennary structures, being about 1 : 3 for K₂tu-PA, 1 : 8 for human colon fibroblast t-PA, 1 : 1.3 for recombinant t-PA [45], and 1 : 4.4 for variant recombinant t-PA [53].

Recombinant and human colon fibroblast t-PA contain in addition to the *N*-acetylglucosamine type, also oligomannose and hybrid type of structures [8, 45, 54]. In K₂tu-PA, the N-linked carbohydrate moiety is fully processed to *N*-acetylglucosamine type of oligosaccharide structures. The absence of oligomannose-type structures may prolong the half-life of K₂tu-PA relative to t-PA, since the uptake from blood circulation by the hepatic mannose receptor is prohibited, so that a lower dose of plasminogen activator may lead to a safer drug policy.

The primary structures of the N-linked carbohydrate moiety of u-PA are not yet elucidated. The carbohydrate chains contain at least four GlcNAc and two GalNAc residues [14]. The O-linked Fuc residue in u-PA [17] and in t-PA [16] was located in the epidermal growth-factor-like domain, which is omitted in the sequence of K₂tu-PA. No evidence has been found for the existence of O-linked fucose or oligosaccharides, by sugar analysis on de-*N*-glycosylated K₂tu-PA-I after gel permeation chromatography.

Oligosaccharide fingerprinting was applied to assess the consistency of the production of K₂tu-PA. The K₂tu-PA-I batch was fermented in a stirred tank bioreactor and was isolated by sequential affinity, cation-exchange, and gel permeation chromatography. The K₂tu-PA-II and -III batches were produced under identical conditions, a year later than the K₂tu-PA-IV batch, and all three batches were produced in a perfusion chemostat bioreactor, and were purified from the culture medium by sequential cation-exchange, anion-exchange, hydrophobic interaction, affinity, and gel permeation chromatography. To avoid contamination, more narrow fractions of K₂tu-PA-II, -III, and -IV were collected as compared to K₂tu-PA-I, purified by immunoaffinity chromatography (cf. Tables 4 and 6), which may explain the relative decrease of mono- and tetrasialylated oligosaccharides. Deviations in oligosaccharide compositions between different recombinant glycoprotein productions are principally addressed to variations in clonal and cell culture conditions. However, the isolation procedure can also play a crucial role in the final microheterogeneity of the carbohydrate structures of an isolated glycoprotein.

Finally, the less processed *N*-acetylglucosamine type of structures at Asn12 in favour of diantennary compounds, as compared to those at Asn247, together with a clear change in the molar ratio of tri- and tri'-antennary compounds in favour of triantennary compounds and the decrease of the relative amount of tetraantennary carbohydrate chains, may indicate a lower susceptibility of the diantennary oligosaccharides at Asn12 towards GlcNAc-transferase V, as compared to the Asn247 glycosylation site [55]. In addition, the partial *N*-glycosylation of Asn12 indicates that this site may be hindered for oligosaccharide-specific processing enzymes.

The authors thank Dr C. Augé (Université Paris-Sud, Orsay, France) for the generous gift of Neu5,9Ac₂α2-6Galβ1-4GlcNAc. This project was financially supported by Ciba-Geigy, the Netherlands Program for Innovation Oriented Carbohydrate Research (IOP-k), and the Netherlands Foundation for Chemical Research (NWO/SOON).

REFERENCES

- Danø, K., Andreasen, P. A., Grøndahl-Hansen, J., Kristensen, P., Nielsen, L. S. & Skriver, L. (1985) Plasminogen activators, tissue degradation, and cancer, *Adv. Cancer Res.* **44**, 139–266.
- Verstraete, M., Bory, M., Collen, D., Erbel, R., Lennane, R. J., Mathey, D., Michels, H. R., Scharl, M., Uebis, R., Bernard, R., Brower, R. W., De Bono, D. P., Huhmann, W., Lubsen, J., Meyer, J., Rutsch, W., Schmidt, W. & Von Essen, R. (1985) Randomised trial of intravenous recombinant tissue-type plasminogen activator versus intravenous streptokinase in acute myocardial infarction, *Lancet* **1**, 842–847.
- Williams, D. O., Borer, J., Braunwald, E., Chesebro, J. H., Cohen, L. S., Dalen, J., Dodge, H. T., Francis, C. K., Knatterud, G., Ludbrook, P., Markis, J. E., Mueller, H., Desvigne-Nickens, P., Passamani, E., Powers, E. R., Rao, A. K., Roberts, R., Ross, A., Ryan, T. J., Sobel, B. E., Winniford, M., Zaret, B. & Co-Investigators (1986) Intravenous recombinant tissue-type plasminogen activator in patients with acute myocardial infarction: a report from the NHLBI thrombolysis in myocardial infarction trial, *Circulation* **73**, 338–346.
- TIMI Study Group (1985) The thrombolysis in myocardial infarction (TIMI) trial: phase I findings, *N. Engl. J. Med.* **312**, 932–936.
- Dawson, K. J. & Hamilton, G. (1991) Recombinant tissue-type plasminogen activator versus urokinase in peripheral arterial occlusions, *Radiology* **178**, 283–284.
- Fears, R. (1989) Binding of plasminogen activators to fibrin: characterization and pharmacological consequences, *Biochem. J.* **261**, 313–324.
- Pohl, G., Källström, M., Bergsdorf, N., Wallén, P. & Jörnvall, H. (1984) Tissue plasminogen activator: peptide analyses confirm an indirectly derived amino acid sequence, identify the active site serine residue, establish glycosylation sites, and localize variant differences, *Biochemistry* **23**, 3701–3707.
- Parekh, R. B., Dwek, R. A., Thomas, J. R., Opendakker, G., Rademacher, T. W., Wittwer, A. J., Howard, S. C., Nelson, R., Siegel, N. R., Jennings, M. G., Harakas, N. K. & Feder, J. (1989) Cell-type specific and site-specific *N*-glycosylation of type I and type II human tissue plasminogen activator, *Biochemistry* **28**, 7644–7662.
- Chan, A. L., Morris, H. R., Panico, M., Etienne, A. T., Rogers, M. E., Gaffney, P., Creighton-Kempford, L. & Dell, A. (1991) A novel sialylated *N*-acetylgalactosamine-containing oligosaccharide is the major complex-type structure present in Bowes melanoma tissue plasminogen activator, *Glycobiology* **1**, 173–185.
- Wittwer, A. J., Howard, S. C., Carr, L. S., Harakas, N. K., Feder, J., Parekh, R. B., Rudd, P. M., Dwek, R. A. & Rademacher, T. W. (1989) Effects of *N*-glycosylation on in vitro activity of Bowes melanoma and human colon fibroblast derived tissue plasminogen activator, *Biochemistry* **28**, 7662–7669.
- Howard, S. C., Wittwer, A. J. & Welply, J. K. (1991) Oligosaccharides at each glycosylation site make structure-dependent contributions to biological properties of human tissue plasminogen activator, *Glycobiology* **1**, 411–417.
- Krause, J. (1988) Catabolism of tissue-type plasminogen activator (t-PA), its variants, mutants and hybrids, *Fibrinolysis* **2**, 133–142.
- Wittwer, A. J. & Howard, S. C. (1990) Glycosylation at Asn-184 inhibits the conversion of single-chain to two-chain tissue-type plasminogen activator by plasmin, *Biochemistry* **29**, 4175–4180.
- Steffens, G. J., Günzler, W. A., Ötting, F., Frankus, E. & Flohé, L. (1982) The complete amino acid sequence of low molecular mass urokinase from human urine, *Hoppe-Seyler's Z. Physiol. Chem.* **363**, 1043–1058.
- McLellan, W. L., Vetterlein, D. & Roblin, R. (1980) The glycoprotein nature of human plasminogen activators, *FEBS Lett.* **115**, 181–184.
- Harris, R. J., Leonard, C. K., Guzzetta, A. W. & Spellman, M. W. (1991) Tissue plasminogen activator has an O-linked fucose attached to threonine-61 in the epidermal growth factor domain, *Biochemistry* **30**, 2311–2314.
- Buko, A. M., Kentzer, E. J., Petros, A., Menon, G., Zuiderweg, E. R. P. & Sarin, V. K. (1991) Characterization of a posttranslational fucosylation in the growth factor domain of urinary plasminogen activator, *Proc. Natl Acad. Sci. USA* **88**, 3992–3996.
- Van Zonneveld, A.-J., Veerman, H. & Pannekoek, H. (1986) Autonomous functions of structural domains on human tissue-type plasminogen activator, *Proc. Natl Acad. Sci. USA* **83**, 4670–4674.
- De Vries, C., Veerman, H., Blasi, F. & Pannekoek, H. (1988) Artificial exon shuffling between tissue-type plasminogen activator (t-PA) and urokinase (u-PA): a comparative study on the fibrinolytic properties of t-PA/u-PA hybrid proteins, *Biochemistry* **27**, 2565–2572.
- Gilbert, W. (1985) Genes-in-pieces revisited, *Science* **228**, 823–824.
- Piérard, L., Quintana, L. G., Reff, M. E. & Bollen, A. (1989) Production in eukaryotic cells and characterization of four hybrids of tissue-type plasminogen activators, *DNA* **8**, 321–328.
- Asselbergs, F. A. M., Bürgi, R., Chaudhuri, B., Heim, J., Meyhack, B., Rajput, B., Van Oostrum, J. & Alkan, S. (1993) Localization of epitopes by monoclonal antibodies on tissue-type and urokinase-type plasminogen activators using recombinant hybrid enzymes, *Fibrinolysis* **7**, 1–14.
- Kamerling, J. P., Hård, K. & Vliegthart, J. F. G. (1990) Structural analysis of carbohydrate chains of native and recombinant-DNA glycoproteins, in *From clone to clinic* (Crommelin, D. J. A. & Schellekens, H., eds) pp. 295–304, Kluwer Academic Publishers, The Netherlands.
- Hokke, C. H., Bergwerff, A. A., Van Dedem, G. W. K., Van Oostrum, J., Kamerling, J. P. & Vliegthart, J. F. G. (1990) Sialylated carbohydrate chains of recombinant human glycoproteins expressed in Chinese hamster ovary cells contain traces of *N*-glycolylneuraminic acid, *FEBS Lett.* **275**, 9–14.
- Asselbergs, F. A. M., Will, H., Wingfield, P. & Hirschi, M. (1986) A recombinant Chinese hamster ovary cell line containing a 300-fold amplified tetramer of the hepatitis B genome together with a double selection marker expresses high levels of viral protein, *J. Mol. Biol.* **189**, 401–411.
- Zimmerman, M., Quigley, J. T., Ashe, B., Dorn, C., Goldfarb, R. & Troll, W. (1978) Direct fluorescent assay of urokinase and plasminogen activators of normal and malignant cells: kinetics and inhibitor profiles, *Proc. Natl Acad. Sci. USA* **75**, 750–753.
- Crestfield, A. M., Moore, S. & Stein, W. H. (1963) The preparation and enzymatic hydrolysis of reduced and *S*-carboxymethylated proteins, *J. Biol. Chem.* **238**, 622–627.
- Damm, J. B. L., Voshol, H., Hård, K., Kamerling, J. P. & Vliegthart, J. F. G. (1989) Analysis of *N*-acetyl-4-*O*-acetylneuraminic-acid-containing *N*-linked carbohydrate chains released by peptide-*N*⁴-(*N*-acetyl-β-glucosaminyl)asparagine amidase F; application to the structure determination of the carbohydrate chains of equine fibrinogen, *Eur. J. Biochem.* **180**, 101–110.
- Laemmli, U. K. (1970) Cleavage of structural proteins during the assembly of the head of bacteriophage T4, *Nature* **227**, 680–685.
- Konradt, T., Schlichting, A., May, B. & Veh, R. W. (1987) Histochemical differentiation between tissue-bound 9-*O*-acetylsialic acid and 7,9-di-*O*-acetyl-sialic acid: periodate oxidation studies with purified 9-*O*-acetyl-sialyllactose from rat urine, *Anat. Anz.* **163**, 159–160.

31. Schauer, R. (1978) Characterization of sialic acids, *Methods Enzymol.* 50, 64–89.
32. Van Pelt, J., Dorland, L., Duran, M., Hokke, C. H., Kamerling, J. P. & Vliegthart, J. F. G. (1990) Sialyl- α -2-6-mannosyl- β -1-4-N-acetylglucosamine, a novel compound occurring in urine of patients with β -mannosidosis, *J. Biol. Chem.* 265, 19 685–19 689.
33. Augé, C., Fernandez-Fernandez, R. & Gautheron, C. (1990) The use of immobilised glycosyltransferases in the synthesis of sialyloligosaccharides, *Carbohydr. Res.* 200, 257–268.
34. Kamerling, J. P. & Vliegthart, J. F. G. (1989) Mass spectrometry, in *Clinical biochemistry; principles, methods, applications*, vol. 1, *Mass spectrometry* (Lawson, A. M., ed.) pp. 175–263, Walter de Gruyter & Co., Berlin.
35. Hara, S., Yamaguchi, M., Takemori, Y., Furuhashi, K., Ogura, H. & Nakamura, M. (1989) Determination of mono-O-acetylated N-acetylneuraminic acids in human and rat sera by fluorometric high-performance liquid chromatography, *Anal. Biochem.* 179, 162–166.
36. Vliegthart, J. F. G., Dorland, L. & Van Halbeek, H. (1983) High-resolution, ^1H -nuclear magnetic resonance spectroscopy as a tool in the structural analysis of carbohydrates related to glycoproteins, *Adv. Carbohydr. Chem. Biochem.* 41, 209–374.
37. Hård, K., Spronk, B. A., Hokke, C. H., Kamerling, J. P. & Vliegthart, J. F. G. (1991) The potency of amide protons for assignments of NMR spectra of carbohydrate chains of glycoproteins, recorded in $^1\text{H}_2\text{O}$ solutions, *FEBS Lett.* 287, 108–112.
38. Hård, K., Van Zadelhoff, G., Moonen, P., Kamerling, J. P. & Vliegthart, J. F. G. (1992) The Asn-linked carbohydrate chains of human Tamm-Horsfall glycoprotein of one male. Novel sulfated and novel N-acetylgalactosamine-containing N-linked carbohydrate chains, *Eur. J. Biochem.* 209, 895–915.
39. Marion, D. & Wüthrich, K. (1983) Application of phase sensitive two-dimensional correlated spectroscopy (COSY) for measurements of ^1H - ^1H spin-spin coupling constants in proteins, *Biochem. Biophys. Res. Commun.* 113, 967–974.
40. Rance, M., Sorensen, O. W., Bodenhausen, G., Wagner, G., Ernst, R. R. & Wüthrich, K. (1983) Improved spectral resolution in COSY ^1H NMR spectra of proteins via double quantum filtering, *Biochem. Biophys. Res. Commun.* 117, 479–485.
41. Marion, D., Ikura, M., Tschudin, R. & Bax, A. (1989) Rapid recording of 2D NMR spectra without phase cycling application to the study of hydrogen exchange in proteins, *J. Magn. Reson.* 85, 393–399.
42. Bax, A. & Davis, D. G. (1985) MLEV-17 based two-dimensional homonuclear magnetization transfer spectroscopy, *J. Magn. Reson.* 65, 355–360.
43. Bothner-By, A. A., Stephens, R. L. & Lee, J. (1984) Structure determination of a tetrasaccharide: transient nuclear Overhauser effects in the rotating frame, *J. Am. Chem. Soc.* 106, 811–813.
44. Hård, K., Mekking, A., Damm, J. B. L., Kamerling, J. P., De Boer, W., Wijnands, R. A. & Vliegthart, J. F. G. (1990) Isolation and structure determination of the intact sialylated N-linked carbohydrate chains of recombinant human follitropin expressed in Chinese hamster ovary cells, *Eur. J. Biochem.* 193, 263–271.
45. Spellman, M. W., Basa, L. J., Leonard, C. K., Chakel, J. A., O'Connor, J. V., Wilson, S. & Van Halbeek, H. (1989) Carbohydrate structures of human tissue plasminogen activator expressed in Chinese hamster ovary cells, *J. Biol. Chem.* 264, 14 100–14 111.
46. Hokke, C. H., Kamerling, J. P., Van Dedem, G. W. K. & Vliegthart, J. F. G. (1991) Determination of the branch location of extra N-acetylglucosamine units in sialo N-linked tetra-antennary oligosaccharides, *FEBS Lett.* 286, 18–24.
47. Breg, J., Kroon-Batenburg, L. M. J., Strecker, G., Montreuil, J. & Vliegthart, J. F. G. (1989) Conformational analysis of the sialyl α (2 \rightarrow 3/6)N-acetylglucosamine structural element occurring in glycoproteins, by 2D-NOE ^1H -NMR spectroscopy in combination with HSEA and MM2HB energy calculations, *Eur. J. Biochem.* 178, 727–739.
48. Dorland, L., Van Halbeek, H., Vliegthart, J. F. G., Schauer, R. & Wiegand, H. (1986) A 500-MHz ^1H -N.M.R. study of oligosaccharides derived from gangliosides by ozonolysis-alkaline fragmentation, *Carbohydr. Res.* 151, 233–245.
49. Weisshaar, G., Baumann, W., Friebolin, H., Brunner, H., Mann, H., Sieberth, H.-G. & Opferkuch, H.-J. (1987) Isolierung und NMR-spektroskopische Charakterisierung sialinsäurehaltiger Verbindungen aus dem Hämofiltrat chronisch urämischer Patienten, *Biol. Chem. Hoppe-Seyler* 368, 647–658.
50. Davidson, D. J. & Castellino, F. J. (1991) Oligosaccharide structures present on asparagine-289 of recombinant human plasminogen expressed in a Chinese hamster ovary cell line, *Biochemistry* 30, 625–633.
51. Schauer, R. (1987) Sialic acids: metabolism of O-acetyl groups, *Methods Enzymol.* 138, 611–626.
52. Schauer, R., Casals-Stenzel, J., Corfield, A. P. & Veh, R. W. (1988) Subcellular site of the biosynthesis of O-acetylated sialic acids in bovine submandibular gland, *Glycoconjugate J.* 5, 257–270.
53. Nimitz, M., Noll, G., Pâques, E.-P. & Conradt, H. S. (1990) Carbohydrate structures of a human tissue plasminogen activator variant expressed in recombinant Chinese hamster ovary cells, *FEBS Lett.* 271, 14–18.
54. Pfeiffer, G., Schmidt, M., Strube, K.-H. & Geyer, R. (1989) Carbohydrate structure of recombinant human uterine tissue plasminogen activator expressed in mouse epithelial cells, *Eur. J. Biochem.* 186, 273–286.
55. Schachter, H. (1986) Biosynthetic controls that determine the branching and microheterogeneity of protein-bound oligosaccharides, *Biochem. Cell. Biol.* 64, 163–181.